Jonckheere-Terpstra test for nonclassical error versus log-sensitivity relationship of quantum spin network controllers

E. Jonckheere, S. Schirmer, and F. Langbein

November 27, 2017

Abstract

Selective information transfer in spin ring networks by energy landscape shaping control has the property that the error $1-\text{prob}$, where prob is the transfer success probability, and the sensitivity of the error to spin coupling uncertainties are statistically increasing across a family of controllers of increasing error. The need for a statistical Hypothesis Testing of a concordant trend is made necessary by the noisy behavior of the sensitivity versus the error as a consequence of the optimization of the controllers in a challenging error landscape. Here, we examine the concordant trend between the error and another measure of performance—the logarithmic sensitivity—used in robust control to formulate a well known fundamental limitation. Contrary to error versus sensitivity, the error versus logarithmic sensitivity trend is less obvious, because of the amplification of the noise due to the logarithmic normalization. This results in the Kendall τ test for rank correlation between the error and the log sensitivity to be somewhat pessimistic with marginal significance level. Here it is shown that the Jonckheere-Terpstra test, because it tests the Alternative Hypothesis of an ordering of the medians of some groups of log sensitivity data, alleviates this statistical problem. This identifies cases of concordant trend between the error and the logarithmic sensitivity, a highly anti-classical features that goes against the well know sensitivity versus complementary sensitivity limitation.

1 Introduction

1.1 Classical robust control bedrock

One of the tenets of classical linear Single Degree of Freedom (SDoF) multivariable control [32] is that the two fundamental figures of merit—tracking error and logarithmic sensitivity to model uncertainty—are in conflict. The former is quantified by the sensitivity matrix $S = (I + L)^{-1}$ and the latter by the complementary sensitivity $T = L(I + L)^{-1}$, where $L(s)$ is the input loop matrix. Specifically,

$$e_{\text{track}}(s) = S(s)r(s),$$

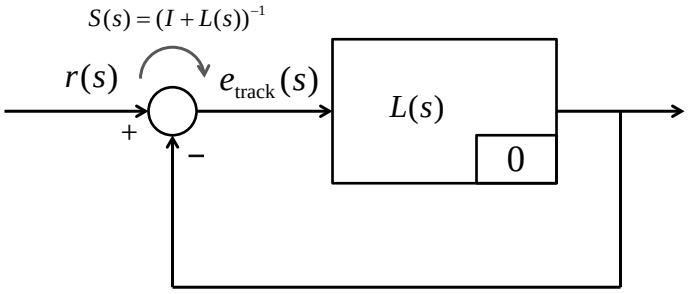

Figure 1: Classical tracking error e_{track} in the classical control architecture

where $r(s)$ is an extraneous reference and $e_{\text{track}}(s)$ is the tracking error, as shown in Fig. 1. $T(s)$ appears in the logarithmic sensitivity of $S(s)$ as $S^{-1}(dS) = (dL)L^{-1}T$. The conflict is obvious from $S + T = I$. The SDoF limitation can be overcome by a 2-Degree of Freedom (2DoF) configuration, as already pointed out by Horowitz [12, Chap. 6] and recently made explicit in [3, 45].

1.2 The quantum state overlap control problem

This paper investigates whether this fundamental limitation survives in the quantum world, more precisely, in spin-$\frac{1}{2}$ networks where fabrication uncertainties at nano-scale make it hard to ensure precise coupling strengths between the spins. The answer is definitely negative for the class of quantum control problems where the objective is to achieve maximum overlap between the controlled wave function $|\Psi_D(t_f)\rangle$ at some final time t_f and some reference or target wave function $|\Psi_{\text{target}}\rangle$. In the preceding, D denotes the controller. The controller belongs to a class of quantum control systems where the controller sole authority is to modify, *in a physically meaningful manner,* the parameters of the Hamiltonian [8]. Even though the basic concepts developed here remain valid for the whole class of such controllers, here, however, we will more specifically consider controllers that induce energy level shifts [5, 15, 16, 17, 18, 24, 33]. More specifically in this paper, $D = \text{diag}\,(D_1, D_2, ..., D_M)$ is a diagonal matrix of bias fields added to the Hamiltonian in some subspace. The concept is illustrated in Fig. 2. In practice, we could envisage, e.g., electron spins in quantum dots whose energy levels can be controlled by voltages applied to surface gates [27].

By "maximum overlap," or "maximum fidelity," we mean

$$\max_{D,t_f} |\langle \Psi_{\text{target}} | \Psi_D(t_f) \rangle| \leq 1, \tag{1}$$

where $\langle \cdot | \cdot \rangle$ denotes the inner product in the complex Hilbert space. The upper bound on the fidelity is easily understood from the Cauchy-Schwartz inequality and the unit norm of the wave function. It turns out that this maximum overlap does not trickle down to the standard tracking problem

$$\min_{D,t_f} \|\Psi_{\text{target}} - \Psi_D(t_f)\|,$$

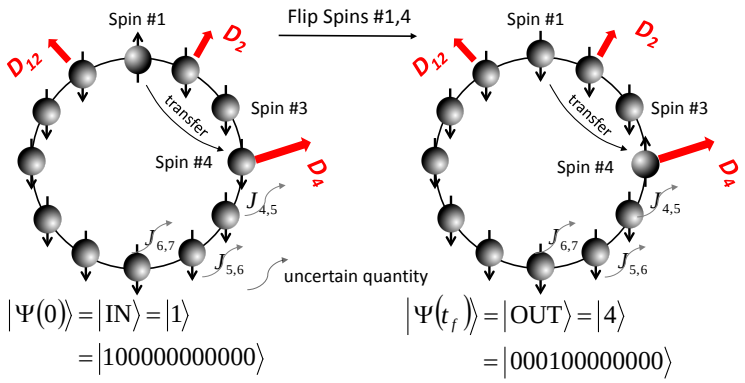

Figure 2: Illustration of the excitation transfer problem. Excitation (spin "up") originally on spin #1 has to be transferred to spin #4. This is accomplished by bias fields $\{D_m\}_{m=1}^{12}$, despite uncertainties on the couplings $J_{m,m+1}$. (Not all bias fields are shown for clarity of the picture.) The initial (target) condition on the wave function Ψ means that the INput (OUTput) excitation is on spin #1 (spin #4).

but to a projective version of the tracking error [33]:

$$\min_{D,t_f,\phi} \|\Psi_{\text{target}} - e^{\jmath\phi}\Psi_D(t_f)\|,$$

where ϕ is the global phase factor—a purely quantum mechanical concept. The classical-quantum discrepancy can now be understood as follows: Under some circumstances, the projective tracking error may be very small, yet the classical tracking error may be so large as to allow for small logarithmic sensitivity.

In the same way as the conventional tracking error leads to a sensitivity matrix $S(s)$, the projective tracking error leads to an unconventional sensitivity matrix [33]. The problem is that this sensitivity matrix does not easily lend itself to an analytical formulation of the limitations on achievable performance. Besides, the challenging landscape in which the optimization (1) has to be conducted relative to both D and t_f leads to ripples in the sensitivity versus error plot, calling for a statistical approach to determine concordance or discordance between the two figures of merit.

1.3 Statistical approach to classical-quantum discrepancy

We consider spin-rings as prototype quantum systems to test our hypothesis of anti-classicality. As shown in Fig. 2, a M-spin ring is an assembly of M spins arranged along a ring with near neighbor coupling $J_{m,m+1}$ of the XX or Heisenberg type. We chose spin rings because they are prototypes of quantum routers [18] that have to transfer a single excitation (spin "up") from one spin to another spin. To achieve this objective, time-invariant but spatially distributed bias fields D_1, D_2, ..., D_M are deployed. Such controller fits in the class of controllers mentioned earlier, as the D_m's appear on the diagonal of the Hamiltonian. With this data, which includes the controller, the

Schrödinger equation can be integrated analytically, and a closed form expression for the fidelity as well as its sensitivity can be derived [33].

The problem is that there is no closed-form solution of the optimization (1). As shown in [24, Fig. 2], the error landscape is extremely challenging, and some optimization runs are successful at finding solutions very close to the upper bound, while the other solutions remain trapped in local minima with poor fidelity. The reward of having a variety of controllers achieving various levels of performance from optimal to poor is that it allows us to check—even quantify—the concordance or discordance between achievable transfer performance and the log sensitivity to the uncertain coupling parameters. This quantification is offered by the Z-statistic of the Kendall τ and more specifically the $|Z|$-statistic of Jonckheere-Terpstra on the data base [25] spanning across all rings from size 3 to 20, all transfers, and all coupling uncertainties.

More specifically, the statistical analysis is done as follows: The controllers $\{D(n)\}_{n=1}^{N}$ from the database [25] are classified by increasing order of the error $\sqrt{1-|\langle\Psi_{\text{target}}|\Psi_{D(n)}(t_f)\rangle|} =: x_n$ they achieve. Define y_n to be the log-sensitivity of the nth controller. Classically, one would expect the sequences $\{x_n\}$ and $\{y_n\}$ to be discordant—that is, the error x_n is increasing while the sensitivity y_n is decreasing with n. Contrary to classical control wisdom, in this quantum set-up the two sequences are concordant—that is, both $\{x_n\}$ and $\{y_n\}$ are increasing. Naturally, in this numerical set-up "concordant" and "discordant" have to be understood in a statistical sense. In general, the larger the $|Z|$-statistic of Jonckheere-Terpstra, the more the sequences are concordant.

The purpose of this paper is to test the Null Hypothesis H_0 of no rank correlation between $\{x_n\}$ and $\{y_n\}$ using the Jonckheere-Terpstra $|Z|$-statistic on the variety of rings, subject the a variety of transfers, under the variety of parameter uncertainties compiled in the dataset [25]. In many cases, as identifed in Sec. 8, H_0 is rejected in favor of the Alternative Hypothesis H_A of concordance of $\{x_n\}$ and $\{y_n\}$.

1.4 Paper outline

The paper is organized as follows: In Section 2, we review the spin network concept, the single excitation subspace, and we define the quantum excitation transport as the problem of having the solution to Schrödinger's equation move from an initial state of excitation to a target state of excitation. In Section 3, the quantum excitation transport is contrasted with classical tracking control. In Section 4, as an alternative to the analytical approach, we introduce the two statistical rank correlation tests—the Kendall τ and the Jonckheere-Terpstra tests— which we propose to investigate whether the error and the logarithmic sensitivity are positively correlated. Section 5 follows formal statistics methods and introduces the Type II error in the test. The statistical results specific to those controllers in the database [25] are presented in Section 6, followed by Section 7, which shows that the power of the Jonckheere-Terpstra test as applied to the specific error versus sensitivity is within statistical gold standards. Finally, in Section 8, we argue that, in excitation transport between nearby spins, classical limitations are overcome, while they tend to survive in case of transport between nearly diametrically opposed spins in rings. Appendix A reviews some variants of the Jonckheere-Terpstra test, Appendix B reviews the left-tailed test, and

Appendix C, the von Neumann (rank) ratio test, is presented as a test for independence of the observations.

1.5 Notation

The notation related to quantum physics is shown by the following table:

Ψ	wave function of quantum ring
H	Hamiltonian of uncontrolled quantum ring in single excitation subspace
D	diagonal control Hamiltonian in single excitation subspace
$\|\text{IN}\rangle$	state of INput excitation into router
$\|\text{OUT}\rangle$	state of OUTput excitation out of router
$J_{m,m+1}$	coupling between spins m and $m+1$
M	number of spins in ring
$D_m(n)$	mth component of bias field of nth optimization run
N	number of fidelity optimization runs
err	error $\sqrt{1-\|\langle\Psi_{\text{target}}\|\Psi_D(t_f)\rangle\|}$
prob	probability of successful transfer $\|\langle\Psi_{\text{target}}\|\Psi_D(t_f)\rangle\|^2$
$\mathbf{X}_m, \mathbf{Y}_m, \mathbf{Z}_m$	Pauli spin matrices of spin m in network
s^x, s^y, s^z	2×2 Pauli matrices of single spin

The notation related to statistics is as follows:

N	sample size of (ring size, transfer, uncertainty) experiment
x_n	independent variable (error 1-prob)) for sample n
y_n	dependent variable ((log)sensitivity) for sample n
I	number of bins in Jonckheere-Terpstra test
i	a specific bin in Jonckheere-Terpstra test
N_i	sample size in bin i
μ, σ^2	mean and variance, resp.
s^2	unbiaised estimate of variance
Z	normally distributed test statistic
JT	$= \|Z\|$, test statistic of Jonckheere-Terpstra
p	$\int_u^\infty f_U(u)du$ where f_U is the test statistic
α	significance level
VN	von Neumann ratio
RVN	rank von Neumann ratio

2 Excitation transport in networks of spins

2.1 Network of spins

The paper deals with the so-called single excitation, that is, a situation where one and only one spin in the network is "up." It is however important to understand how this concept emerges from the general situation where as many as M spins could be

excited. The total Hamiltonian (including the controller) of a spin ring as the one shown in Fig. 2 is given by

$$\sum_{m=1}^{M} J_{m,m+1}(\mathbf{X}_m\mathbf{X}_{m+1} + \mathbf{Y}_m\mathbf{Y}_{m+1} + \varepsilon\mathbf{Z}_m\mathbf{Z}_{m+1}) + \sum_{m=1}^{M} D_m\mathbf{Z}_m. \tag{2}$$

In the above, $\mathbf{X}_m$, $\mathbf{Y}_m$, $\mathbf{Z}_m$ are the Pauli x, y, z operators, respectively, of the spin m in the ring, with the convention that $(\mathbf{X},\mathbf{Y},\mathbf{Z})_{M+1} = (\mathbf{X},\mathbf{Y},\mathbf{Z})_1$ to enforce the ring structure. More specifically,

$$(\mathbf{X},\mathbf{Y},\mathbf{Z})_m = I_{2\times 2}^{\otimes(m-1)} \otimes s^{(x,y,z)} \otimes I_{2\times 2}^{\otimes(M-m)},$$

where $s^{(x,y,z)}$ are the Pauli spin matrices

$$s^x = \begin{pmatrix} 0 & 1 \\ 1 & 0 \end{pmatrix},\ s^y = \begin{pmatrix} 0 & -\jmath \\ \jmath & 0 \end{pmatrix},\ s^z = \begin{pmatrix} 1 & 0 \\ 0 & -1 \end{pmatrix}.$$

$J_{m,m+1} = J_{m+1,m}$ is the coupling strength between spins m and $m+1$, with the convention that with $J_{M,M+1} = J_{M,1}$. Should $\varepsilon = 0$ in the Hamiltonian, the ring is said to be XX, while it is said to be Heisenberg if $\varepsilon = 1$.

The operator $\mathbf{Z} = \frac{1}{2}\sum_{m=1}^{M}(I + \mathbf{Z}_m)$ counts the number of spins that are in the excited state. Since $\mathbf{Z}$ commutes with the Hamiltonian, the number of such spins remains invariant under the total motion. Define the single excitation subspace as the eigenspace of the $+1$ eigenvalue of $\mathbf{Z}$. In this single excitation subspace, the Hamiltonian of the M-ring reduces to the $M \times M$ Hermitian matrix

$$H + D = \begin{pmatrix} D_1 & J_{1,2} & 0 & \dots & 0 & J_{1,M} \\ J_{1,2} & D_2 & J_{2,3} & & 0 & 0 \\ 0 & J_{2,3} & D_3 & & 0 & 0 \\ \vdots & & \ddots & \ddots & \ddots & \\ 0 & 0 & 0 & & D_{M-1} & J_{M-1,M} \\ J_{1,M} & 0 & 0 & \dots & J_{M-1,M} & D_M \end{pmatrix} \tag{3}$$

and the wave function $\Psi \in \mathbb{C}^M$ is solution of the reduced Schrödinger equation

$$|\dot{\Psi}(t)\rangle = -\jmath(H + D)|\Psi(t)\rangle, \quad \Psi(0) = |\mathrm{IN}\rangle. \tag{4}$$

2.2 Quantum transport control

In Eq. (4), D could be time-invariant, time-varying, may or may not involve measurement feedback, the important point being that it should achieve high fidelity excitation transfer even in the presence of some uncertainties in H. By a well known, even fundamental, control paradigm that goes back to Bode, the latter can only be achieved if D creates a feedback, possibly "hidden," that wraps around the uncertainty. As already pointed out by Kosut [22], quantum gates can achieve both high fidelity operation and robustness with open-loop control, because the apparently "open-loop" control creates a hidden feedback. This new paradigm can probably be best understood by splitting

the open-loop D-controlled Schrödinger equation (4) as a feedforward dynamics and a feedback control:

$$\begin{aligned} |\dot{\Psi}(t)\rangle &= -\jmath H|\Psi(t)\rangle + u(t), \quad \Psi(0) = |\mathrm{IN}\rangle, \\ u(t) &= -\jmath D|\Psi\rangle(t). \end{aligned} \tag{5}$$

It clearly follows that, even when D does not involve measurements as in [33], Eq. (4) still involves some feedback that may be qualified as "hidden" or better, "field mediated," hence justifying the robustness properties.

In the definition [8] of quantum control as *"tuning quantum interactions between matter and field, or field-field interaction"*, the D-controller would fall in the first category as, e.g., the electric fields from the gate electrodes control the energy levels of electrons in quantum dots. Here, as in [8], the D-controller is taken time-invariant, but spatially varying. In [8], the spatially varying controller is implemented by spatially modifying the dielectric constant of the medium of a wave guide. This has some commonality with our spatially varying bias field approach; however, our D-controller approach seems more related to the DiVincenzo architecture [27].

The drawback, however, of feed-backing $|\Psi(t)\rangle$ rather than the classical error $\Psi_{\text{target}} - |\Psi(t)\rangle$ is that the controller has to be *selective*, that is, it must incorporate the knowledge of Ψ_{target}, for otherwise the system has no way of knowing where to go.

From the pure linear algebra viewpoint, observe that Eq. (5) can be viewed as a linear feedback design, but a highly nonclassical one, as pointed out by Nijmeijer [28]. Indeed, the diagonal structure of D takes the design outside the classical controllability pole placement problem and furthermore, because of the Hermitian property of H and D, the poles can only be placed on the imaginary axis.

3 Tracking error formulation of quantum spin excitation transport

The excitation transport problem can, in some sense, be viewed as the problem of having $|\Psi(t)\rangle$ track $|\mathrm{OUT}\rangle$. However, there are significant discrepancies between classical and quantum tracking control. First of all, the fundamental quantum figure of merit is not some error but the probability of successful transport of the excitation, or squared fidelity, $|\langle \mathrm{OUT}|\Psi(t_f)\rangle|^2$, where t_f is the time at which the excitation is read out. To simplify the exposition, assume that the probability achieves its maximum, $|\langle \mathrm{OUT}|\Psi(t_f)\rangle|^2 = 1$, in which case it is easily seen that $|\Psi(t_f)\rangle = e^{-i\phi(t_f)}|\mathrm{OUT}\rangle$, or equivalently $|\Psi(t_f)\rangle - e^{-i\phi(t_f)}|\mathrm{OUT}\rangle = 0$ for some global phase factor $\phi(t_f)$. More generally, it is not difficult to show that

$$\Big\| |\mathrm{OUT}\rangle - e^{\jmath\phi(t_f)}|\Psi(t_f)\rangle \Big\|^2 = 2\underbrace{(1 - |\langle \mathrm{OUT}|\Psi(t_f)\rangle|)}_{\mathrm{err}^2(t_f)}, \tag{6}$$

for

$$\phi(t_f) = -\angle\langle \mathrm{OUT}|\Psi(t_f)\rangle.$$

It thus appears that the quantum transport problem of maximizing $|\langle \mathrm{OUT}|\Psi(t_f)\rangle|$ or its "windowed" version $\frac{1}{\delta t}\int_{t_f-\delta t/2}^{t_f+\delta t/2}|\langle \mathrm{OUT}|\Psi(t)\rangle|dt$ is equivalent to minimizing some "tracking error" with the discrepancy that it is not required that the difference between the current state and the target state be small in the ordinary sense, but small in the sense of $\min_\phi \||\mathrm{OUT}\rangle - e^{i\phi}\Psi(t_f)\|$. The latter is related to the Fubini-Study metric [10, p. 31] on the complex projective space $\mathbb{CP}^{M-1}$.

We will refer to the left-hand side of Eq. (6) as the *projective tracking error.*

3.1 Classical-quantum controller structure discrepancies

The hidden feedback

$$u(t) = -\jmath D|\Psi(t)\rangle \tag{7}$$

formulation of the "open-loop" controlled Schrödinger equation (4) where D is a diagonal matrix of spatially distributed biases makes the controller linear, as opposed to bilinear [9, 28]. Conceptually D could still be time-varying, but here we focus on a time-invariant design. As already said, in the latter, case the controller is linear time-invariant, but in the nonclassical sense of [28]. Yet another departure from classical control is that the controller is *selective,* that is, D depends on both $|\mathrm{IN}\rangle$ and $|\mathrm{OUT}\rangle$. $|\mathrm{IN}\rangle$ is the initial condition and, more importantly, $|\mathrm{OUT}\rangle$ is to be interpreted as the reference. The controller is not driven by the tracking error, but depends on *both* the current state and the target state; from this point of view, the controller is of the 2DoF configuration.

Note that, because of the symmetry of the ring, $D(|\mathrm{IN}\rangle, |\mathrm{OUT}\rangle)$ depends only on the *distance* between $|\mathrm{IN}\rangle$ and $|\mathrm{OUT}\rangle$.

Last but not least, the unitary evolution has the property that the controller is not asymptotically stable. Indeed, let D be a controller that achieves $\||\mathrm{OUT}\rangle - e^{-\jmath(H+D)t}|\mathrm{IN}\rangle\| \le \epsilon$. Take an initial state $|\mathrm{IN}\rangle'$ nearby $|\mathrm{IN}\rangle$, that is, $\||\mathrm{IN}\rangle - |\mathrm{IN}\rangle'\| = \eta$. Using the unitary property of the evolution and the triangle inequality, we derive

$$\begin{aligned}
\eta &= \|e^{-\jmath(H+D)t}(|\mathrm{IN}\rangle - |\mathrm{IN}\rangle')\| \\
&= \|(e^{-\jmath(H+D)t}|\mathrm{IN}\rangle - |\mathrm{OUT}\rangle) + (|\mathrm{OUT}\rangle - e^{-\jmath(H+D)t}|\mathrm{IN}\rangle')\| \\
&\le \epsilon + \||\mathrm{OUT}\rangle - e^{-\jmath(H+D)t}|\mathrm{IN}\rangle'\|,
\end{aligned}$$

which yields

$$\||\mathrm{OUT}\rangle - e^{-\jmath(H+D)t}|\mathrm{IN}\rangle'\| \ge \eta - \epsilon.$$

Thus, for an infinitesimally accurate controller ($\epsilon \downarrow 0$), the perturbed state will remain away from the target $|\mathrm{OUT}\rangle$. The latter has the consequence that the controller is not a classical asymptotically stabilizing controller; it is only Lyapunov stable. The latter property means that the state remains localized and won't diffuse. This means that in some cases [5] our controller achieves *Anderson localization* [2, 13, 23].

With these significant departures from classicality, one wonders whether the fundamental error versus log sensitivity limitation is still in force. The problem is that the phase factor appearing in the quantum tracking error does not lead to a classical sensitivity function. In [33], a sensitivity matrix $\mathcal{S}(s)$ was defined via the Laplace

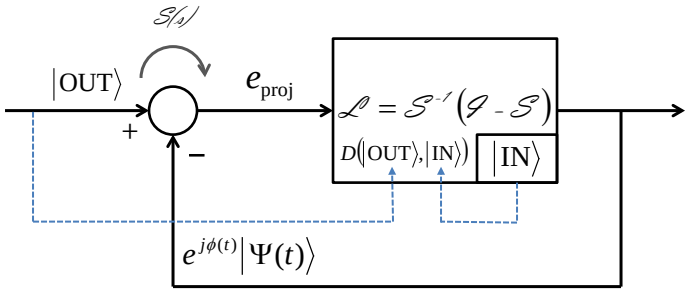

Figure 3: Projective error $|\mathrm{OUT}\rangle - e^{j\phi(t)}|\Psi(t)\rangle$. Note that, contrary to the classical case of Fig. 1, the sensitivity matrix $\mathcal{S}$ is first defined, from which the fictitious loop function $\mathscr{L}$ is defined. The loop matrix is initialized with $|\mathrm{IN}\rangle$. The dotted paths are nonclassical and indicate that the gain D depends on both $|\mathrm{IN}\rangle$ and $|\mathrm{OUT}\rangle$.

transform $\hat{\mathscr{L}}$ of the projective tracking error as

$$\hat{\mathscr{L}}(|\mathrm{OUT}\rangle 1(t) - e^{i\phi(t)}\Psi(t)) = \mathcal{S}(s)|\mathrm{OUT}\rangle \tag{8}$$

for $\phi(t)$ achieving the minimum of $\||\mathrm{OUT}\rangle - e^{i\phi(t)}\Psi(t)\|$. This sensitivity operator takes the form

$$\mathcal{S}(s) = \frac{1}{s}I - \hat{\mathscr{L}}\left[e^{i\phi(t)}\right] * (sI + \jmath(H + D))^{-1} P$$

where P is a permutation such that $P|\mathrm{OUT}\rangle = |\mathrm{IN}\rangle$ and $*$ denotes the complex domain convolution [33]. A clear relationship between $\mathcal{S}(s)$ and its sensitivity to parameters J (a generic notation for $J_{k,k+1}$) in H cannot be expected. For this reason, we propose a statistical approach based on a great many numerical optimization experiments.

Note that, here, we define a sensitivity matrix without proceeding from a loop matrix as done classically. However, a fictitious loop matrix can be defined as

$$\mathscr{L} = \mathcal{S}^{-1}(I - \mathcal{S})$$

and plugged in the feedback diagram of Fig. 3. Clearly, the conventional architecture is recovered, but for a very special loop matrix that embodies the projectivization of the error.

From (8), it is clear that the sensitivity of the sensitivity $\mathcal{S}$ relative to J amounts to sensitivity of err as defined by (6). From the classical control viewpoint, the log-sensitivity is

$$\frac{d\mathrm{err}}{dJ}\frac{1}{\mathrm{err}} = -\frac{1}{4}\frac{1}{\sqrt{\mathrm{prob}}}\frac{d\mathrm{prob}}{dJ}\frac{1}{1-\sqrt{\mathrm{prob}}}.$$

The right-hand side is easily derived from the definition of err taken from (6). If $\mathrm{prob} \approx 1$, as the data base [25] retains only those controllers with an error not exceeding 0.1, then the above can be approximated as

$$\frac{d\mathrm{err}}{dJ}\frac{1}{\mathrm{err}} \approx -\frac{1}{4}\frac{d\mathrm{prob}}{dJ}\frac{1}{(1-\sqrt{\mathrm{prob}})}\frac{2}{(1+\sqrt{\mathrm{prob}})} = -\frac{1}{2}\frac{d\mathrm{prob}}{dJ}\frac{1}{1-\mathrm{prob}}$$

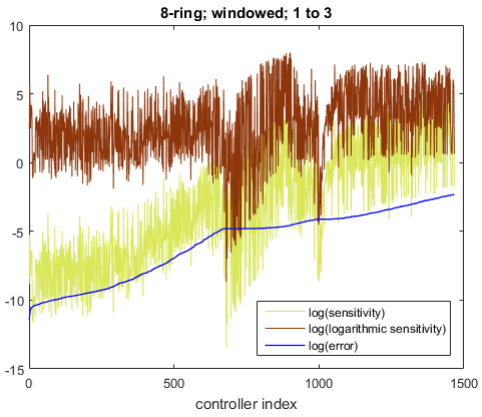

Figure 4: Sensitivity versus logarithmic sensitivity. While the sensitivity is increasing with the error with a Kendall τ of 0.6153, the behavior of the log-sensitivity is less trivial; nevertheless the Jonckheere-Terpstra test rejects the hypothesis of nonincrease of the log-sensitivity.

4 Methods—Type I error

4.1 Overview

Here, as a first step towards an understanding of the error versus sensitivity issue, we proceed numerically by comparing the error $1 - |\langle \mathrm{OUT}|\Psi(t)\rangle|^2$ and its (logarithmic) sensitivity to modeling uncertainties in H across a variety of controllers with error not exceeding 0.1 (see [25] for the data). Precisely, we considered *all* rings from $M = 3$ to $M = 20$ spins together with *all* transfers between any two spins. However, by symmetry, we can restrict ourselves to $|\mathrm{IN}\rangle = |1\rangle$. The study therefore amounts to a total of 108 case-studies, where a case-study is defined by a number of spins M and an $|\mathrm{OUT}\rangle$ spin. For every $M \in [2, 3, \ldots, 19, 20]$ and every $(|\mathrm{IN}\rangle = 1, |\mathrm{OUT}\rangle \leq \lceil M/2 \rceil)$ pair, controllers D were computed by numerical optimization runs of $1-|\langle \mathrm{OUT}|e^{-i(H+D)t_f}|\mathrm{IN}\rangle|^2$ relative to D, t_f, either at the precise time t_f or over a window around t_f, and controllers were ordered by increasing error, as explained in [24, 33] and as illustrated in Fig. 4. Given a case-study $(M, |\mathrm{OUT}\rangle)$ out of a total number of 108 case-studies, the number N of time-windowed optimization runs, or controllers, were between 114 and 1998, with an average of 939 controllers.

Note that we do not have a sampling of the set of *all* controllers. The set of controllers is the subset of those locally optimal controllers computed by the search algorithm and achieving an error not exceeding 0.1.

The major difficulty is that the challenging error landscape and the potential for the solution to be trapped in some local minimums make the (absolute and logarithmic) sensitivity versus error plots quite noisy, as shown by Fig. 4, where controllers are ordered by increasing error. Despite this noisy behavior, the graph of Fig. 4 suggests a positive correlation between the sensitivity and the error (for this particular example). This observation is consistent with classical control; it is indeed easily seen that $dS = -S(dL)S$, meaning that if the error vanishes ($S = 0$) so does the sensitivity ($dS =$

0). However, the correlation between the logarithmic sensitivity $\left|\frac{d\text{prob}}{dJ}\frac{1}{1-\text{prob}}\right|$ relative to J-coupling uncertainties in H and the error is not so obvious. In order to make an *objective* statement about whether the logarithmic sensitivity versus error plot is increasing, decreasing, or inconclusive, we used two rank correlation test statistics: the Kendall τ [20] and the Jonckheere-Terpstra statistic [14, 39].

4.2 Kendall τ

Given a set of independent, dependent variables pairs $\{(x_n, y_n)\}_{n=1}^N$, where $\{x_n\}_{n=1}^N$, $\{y_n\}_{n=1}^N$ are samples of random variables $\mathbf{x}$, $\mathbf{y}$, resp., the (estimate of the) Kendall τ is

$$\tau = \frac{\text{number of concordant pairs} - \text{number of discordant pairs}}{N(N-1)/2} \in [-1, 1],$$

where a concordant pair is typically $((x_k < x_\ell), (y_k < y_\ell))$ and a discordant pair is $((x_k < x_\ell), (y_k > y_\ell))$. The preceding assumes that there are no ties [36]. A Kendall tau in $(0, 1]$ means that the plot of y versus x is increasing—in the control context where $\mathbf{x}$ is the error and $\mathbf{y}$ the sensitivity, small (large) error implies small (large) sensitivity, a bit against traditional control wisdom.

The mean and variance of Kendall τ are, respectively [41],

$$\mu_\tau = 0, \quad \sigma_\tau^2 = \frac{2(2N+5)}{9N(N-1)}.$$

For large data set, the τ statistic

$$Z_\tau = \frac{\tau}{\sigma_\tau}$$

is approximately normal, from which a test of significance can be drawn [1].

A crucial condition is that the samples $\{y_n\}_{n=1}^N$ of $\mathbf{y}$ must be independent. This assumption can be justified by the randomness of the numerical optimizer running in an extremely complicated error landscape. In case of "persistent data," there is a tendency towards an inflated value of the variance of τ [11].

For the error versus sensitivity averaged over a small interval around t_f, the average Kendall τ over *all* rings from 3 to 20 spins and *all* transfers is 0.4535, indicating positive correlation, with a standard deviation of 0.2113, with an average p of 0.001115741. However, for the logarithmic sensitivity, we obtained the less convincing values $\mu(\tau) = 0.1925$ and $\sigma_\tau = 0.2503$, with an average p of 0.338925.

The issue with the Kendall τ is that, when it comes to the data y increasing in an oscillatory fashion under an increase of x, the Kendall τ will find quite a few discordant pairs, even when on an average y is obviously increasing. One remedy would be to smooth over y and rerun the Kendall τ with the smoothed data. This of course would lead to a τ depending on the way the y data has been smoothed over. Here we propose a different solution. The range of values of x is decomposed in a certain number of groups, or "bins," and a Kendall τ like counting is made between groups, but not inside groups. This removes some of the discordant pairs and lead to a better figure of merit. This is the gist of the (nonparametric) Jonckheere-Terpstra test as it is applied to the present robust control problem.

4.3 Jonckheere-Terpstra test

Consider an independent variable, here the error $x = 1-\text{prob}$ where prob is the transfer success probability, and a dependent variable, here the logarithmic sensitivity of the probability relative to coupling errors $y = \left| \frac{d\text{prob}}{dJ} \frac{1}{1-\text{prob}} \right|$, where J is the near-neighbor spin coupling strength. (Note that $1 - \text{prob}$ is not the same error as err, but this does not matter as the Jonckheere-Terpstra test is nonparametric, that is, it does not depend on the values but on the ranking of such values.) We want to show that $y(x)$ is statistically an increasing function ("positive correlation" between x and y.) The range of values of $x = 1 - \text{prob}$ is decomposed in a certain number of groups such that the independent variable increases along the groups. To be formal, consider a partitioning of the values of the independent variable

$$\{x_n\}_{n=1}^N = X_1 \sqcup X_2 \sqcup ... \sqcup X_I$$

such that $\forall x_k \in X_i$, $\forall x_\ell \in X_j$ with $i < j$, we have $x_k \leq x_\ell$ with at least one strict inequality. With this grouping of the values of the independent variable, we construct a grouping of the corresponding values of the dependent variable:

$$\{y_n\}_{n=1}^N = Y_1 \cup Y_2 \cup ... \cup Y_I, \quad Y_i := y(X_i).$$

In each group of dependent variables, we compute the *median* of the population:

$$\widetilde{Y}_1,\ \widetilde{Y}_2,\ ...,\ \widetilde{Y}_I.$$

In the Jonckheere-Terpstra test [14, 39], the Null Hypothesis is

$$H_0 : \widetilde{Y}_1 = \widetilde{Y}_2 = ... = \widetilde{Y}_I$$

and the Alternative Hypothesis is

$$H_A : \widetilde{Y}_1 \leq \widetilde{Y}_2 \leq ... \leq \widetilde{Y}_I, \quad \text{with at least a strict inequality.}$$

The Jonckheere-Terpstra is a test for the Alternative Hypothesis. It is robust and avoids the noise in the log sensitivity because it argues on the medians. (The difficult part, though, is how to group the values of $1 - \text{prob}$.)

The statistic is derived from a counting of the number of cases favorable to the increasing property of y relative to x (the number of concordant pairs in the Kendall tau language). Precisely, we start with the Mann-Whitney U-statistic associated with the pair (i, j) of groups:

$$U_{ij} = \sum_{k=1}^{N_i} \sum_{\ell=1}^{N_j} \Phi(Y_j(\ell) - Y_i(k)), \quad i < j, \tag{9}$$

where

$$\Phi(z) = \begin{cases} 1 & \text{if} \quad z > 0 \\ 1/2 & \text{if} \quad z = 0 \\ 0 & \text{if} \quad z < 0 \end{cases} \quad \text{(ties are counted as 1/2)}$$

and $N_i = |Y_i|$ and $Y_i(k)$ denotes the kth element in Y_i. Defining $U = \sum_{i<j} U_{ij}$, the Jonckheere-Terpstra (JT) standardized test statistic [1] is JT $= |Z|$, where

$$Z = \frac{U - \mu_U}{\sigma_U}.$$

Assuming that there are no ties [26], the mean and the variance are, respectively [6],

$$\begin{aligned} \mu_U &= \frac{N^2 - \sum_{i=1}^{I} N_i^2}{4}, \\ \sigma_U^2 &= \frac{N^2(2N+3) - \sum_{i=1}^{I} N_i^2(2N_i+3)}{72}, \end{aligned} \tag{10}$$

where $N = \sum_{i=1}^{I} N_i$. For a large data set, Z is approximately normally distributed, from which the one-tailed p-value is computed as

$$\begin{aligned} p &= \int_u^\infty f_U(u)du, \quad (u > 0) \\ &= \frac{1}{2}\left(\int_z^\infty f_Z(z)dz + \int_{-\infty}^{-z} f_Z(z)dz\right), \quad (z > 0) \\ &= \frac{1}{2}\left(1 - \mathrm{erf}\left(\frac{z}{\sqrt{2}}\right)\right), \quad (z > 0) \\ &= 1 - \frac{1}{2}\mathrm{erfc}\left(-\frac{\mathrm{JT}}{\sqrt{2}}\right), \quad (\mathrm{JT} = |z|). \end{aligned} \tag{11}$$

The various steps to compute U, Z, and p from the $\{Y_i\}_{i=1}^{I}$ data are implemented in the Matlab function `JTtrend.m` (see [7]), of which we have borrowed the notation.

The Null Hypothesis H_0 of no trend is rejected if $p < \alpha$, where α is the significance level (by default 0.05) and accepted if $p > \alpha$. Equivalently, H_0 is rejected if JT $>$ JT$_\alpha$ and accepted otherwise. The critical value JT$_{\alpha=0.05} \approx 1.6557$ is easily verified from (11). If the Null Hypothesis holds with f_Z normally distributed, $\alpha = 0.05$ is the probability of wrongfully rejecting H_0; this is the Type I error.

Remark: There are other tests revolving around other ways to define the U-statistic. These are quickly reviewed in Appendix A.

Remark: Note that in the case the classical limitations are likely to hold, the left-tailed Jonckheere-Terpstra test should be implemented; see Appendix B.

4.4 Domain of validity of Jonckheere-Terpstra test

There are some conditions for the Jonckheere-Terpstra test to be applicable:

1. **Independence of observations:** The requirement is that for each $(M, |\mathrm{OUT}\rangle)$ case-study the log-sensitivity "observations" $\{y_n\}$ should be independent within each group and across all groups. This is empirically justified

[1] Note that in the original Jonckheere paper [14, Eq. 1] the statistic is rather defined, in our notation, as $U = \sum_{j=i+1} U_{ij}$. The $U = \sum_{i<j} U_{ij}$ is the formulation of the original paper by Terpstra [39, Eq. 3.1]. The Matlab `JTtrend` function [7] follows the latter formulation.

in Section 6.1.1, where an argument based on the dynamics of the optimization algorithm that generates the data $\{y_n\}$ is developed. However, from the austere viewpoint of the mere data $\{y_n\}$ without reference as to how they were generated, this is the issue of securing some randomness in a series of observations, a problem that goes back to von Neumann [42]. This is relegated to Appendix C.

2. **Same group distribution shape:** The distributions of observations in each group must have the same shape and variability. This allows the Jonckheere-Terpstra test to be a test on the medians. Naturally, since we hope to find a trend in the data, this cannot hold true without some preprocessing, typically the removal of the mean. For example, looking at Fig. 6, it is clear that removing the means over appropriate windows ("bins") will give equally distributed log-sensitivity data across the many windows ("bins"). The situation is somewhat more complicated in Fig. 7, where it is critical to correctly place the bins to secure consistent probability densities across the bins. Formally, the empirical cumulative distributions of the $\{y_{n_i} - \bar{y}_i\}$ data inside all bins should be compared. (See Section 6.1.2.)

4.5 Combining test statistics from independent experiments

Let $(\mathrm{JT}_\eta, p_\eta)$ be the test statistic of the experiment η, that is, the JT-statistic and the p value across a variety of controllers for a given number M of spins and a given transfer $|\mathrm{IN}\rangle \to |\mathrm{OUT}\rangle$. (For Jonckheere-Terpstra, we would include the number of bins I in the experiment data.) JT_η and p_η already allow for a Hypothesis Testing (accept or reject classical limitations) *for the given experimental set-up.* However, we want to do a Hypothesis Testing that transcends the particular experimental set up where the number of spins and the transfer are fixed. We want to do a Hypothesis Testing that spans across the many ring sizes and the many possible transfers. If the various experiments were Z-scored with Z normally distributed (as in the Kendall τ), the correct way to combine the various Z_η's would be Stouffer's method [21, 37, 40], $Z = (1/\sqrt{E}) \sum_{\eta=1}^{E} Z_\eta$, since the resulting Z is normally distributed, from which the p is easily computed via (11). A more intuitive way is Liptak's test [21], $Z = (1/E) \sum_{\eta=1}^{E} Z_\eta$. (The Fisher test [44], $p = -2 \sum_{\eta=1}^{E} \log p_\eta$, directly combines the p's.) The problem is that the Jonckheere-Terpstra test is $|Z|$-scored, not Z-scored. Here, we somewhat heuristically follow the Liptak method of just averaging the $|Z|$'s and the p's and verifying from the data of Table 1 that the relation (11), with JT and p replaced by their means, holds up to several decimals. For the deployment of the Stouffer method, the reader is referred to [31].

5 Methods—Type II error and power of test

The U and the $|Z|$-statistics of Section 4.3 hold true under the Null Hypothesis H_0 of no trend. Therefore, α as set to 0.05 is the probability of making the Type I error of rejecting H_0 when it holds true. If we admit that this Type I error is small enough,

under the rejection of H_0, we would favor *some* Alternative Hypothesis H_A. Instead of admitting the normal distribution $f_Z(z) = \frac{1}{\sqrt{2\pi}} \exp(-z^2/2)$ as true under H_0, we now shift the distribution to the right, $f_Z\left(z - \mu^A_{|Z|}\right)$, $\mu^A_{|Z|} > 0$, and admit that the latter holds true under the Alternative Hypothesis. We then define the Type II error, β_α, as the probability of failure to reject the Null Hypothesis when the specific Alternative Hypothesis holds:

$$\beta_\alpha\left(\mu^A_{|Z|}\right) = \int_{-\infty}^{Z_\alpha} f_Z\left(z - \mu^A_{|Z|}\right) dz = 1 - \frac{1}{2}\mathrm{erfc}\left(\frac{Z_\alpha - \mu^A_{|Z|}}{\sqrt{2}}\right). \tag{12}$$

The power of the test given the Type I error α is defined as $1-\beta_\alpha\left(\mu^A_{|Z|}\right)$. Naturally, it depends on the admissible Type I error α and the conjectured $\mu^A_{|Z|}$ defining H_A, but it also depends on the overall sample size N and the population N_i of the bins. Since the $\mu^A_{|Z|}$ is guessed but otherwise a priori unknown, it is essential to assess the power of the test over all realistic $\mu^A_{|Z|}$'s. Usually, we require the power of a test to be 80%.

6 Results—Type I error

6.1 Conditions for test to be applicable

6.1.1 Independence of observations

Here the observations are essentially the many (log)sensitivities achieved by the D-controllers obtained by running the optimization algorithm in the error landscape. We provide an intuitive justification of the independence of the observations, relegating the formal statistical argument to Appendix C.

The initial values chosen for the optimization of the fidelity relative to D are a random sampling of the domain of controllers. In most cases, the difference between the initial D-value and the maximum fidelity D-solution is small. Therefore, it appears that the random sampling should result into a random sampling over the attraction domains for the optimization algorithm. However, if the size of the domain of attraction is notably larger than the mesh of the random sampling of the space of controllers, then there is a bias. If not, then the random initial value sampling matches a random sampling of the maximum fidelity locally optimal controllers. Numerical experiments seem to indicate that the same controller is not found twice over the runs. So this would indicate that the attraction domains are much smaller than the sampling density and that a random sampling of the space of initial controllers should lead to a random sampling of the resulting sensitivity/error data.

It should be noted that contrary to time-series the "time-stamp" n assigned to be observations is not really a time. This can be explained by the way the results were derived. 2000 independent optimization tasks were created for each "case-study," defined by a number of spins M and a target spin $|\mathrm{OUT}\rangle$. These were sent to a cluster and executed in parallel, such that the sequence in which the results came out actually purely depends on the cluster cores and the scheduler used. Tasks were

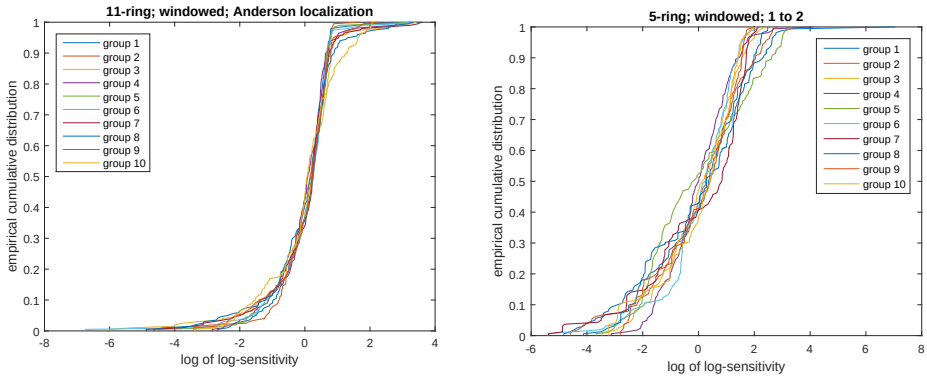

Figure 5: Consistency of empirical cumulative distributions of observations divided in 10 groups of log-sensitivity data. Left: 11-ring with localization at $|1\rangle$; right: 5-ring with $|1\rangle \to |2\rangle$ transfer. The data before grouping is shown in Fig. 6 and Fig. 7, resp.

all mixed across all problems, with some rerun if a machine went down, etc. Each individual task selected an independent initial bias diagonal D-controller and initial time according to a uniform distribution. So, the initial values were iid (using Matlab's pseudo-random number generator) and as already argued this should lead to random (log)sensitivity results.

6.1.2 Empirical cumulative distribution

Computation of the empirical cumulative distributions of the $\{y_n - \bar{y}_i\}_{n=1}^{N_i}$ data inside every bin after removal of the bin mean $\bar{y}_i = (1/N_i)\sum_{n=1}^{N_i} y_n$ reveal that they are fairly consistent. Sample results are shown in Fig. 5, where the partition of the data is uniform in (N/I)-observation groups, except for the last group. In geneal, the empirical cumulative distributions can be made closer by more careful grouping.

6.2 Statistical analysis of error versus log-sensitivity relation

Here we consider all case-studies of rings with $M = 3$ to $M = 20$ spins, with transport $|\text{IN}\rangle = |1\rangle \to |\text{OUT}\rangle$, with $|\text{OUT}\rangle$ ranging from $|1\rangle$ (Anderson localization) to $\lceil \frac{M}{2} \rceil$. This totals to an amount of 108 cases. By symmetry, this covers all cases of transfer of excitation from any spin to any other spin in networks of $M = 3, 4, \cdots, 20$ spins.

In each case-study among the 108 cases, we have N pairs $\{x_n, y_n\}_{n=1}^{N}$. The nth value of the independent variable x_n is the log of the error, $\log(1 - \text{prob}_n)$, where prob_n is the probability of successful $|\text{IN}\rangle \to |\text{OUT}\rangle$ transfer of the nth controller. (The log of the error allows for clearer graphing of the results yet it does not affect the ranking.) The errors are in increasing order $x_k \leq x_\ell$ for $k < \ell$. The dependent variable takes

Table 1: Analysis of the JT := $|Z|$ Jonckheere-Terpstra statistic over whole data base [25] (The $\min p = 0$ is up to 4 decimals.)

I	$\min \mathrm{JT}$	$\bar{\mathrm{JT}}$	$\max \mathrm{JT}$	s_{JT}	$\min p$	$\bar{p}$	$\max p$	s_p
3	0.0472	11.3055	33.0028	11.1729	0	0.0617	0.4812	0.1182
10	0.0433	12.1213	34.7227	12.1481	0	0.0595	0.4827	0.1156
100	0.364	12.2425	35.0389	12.3419	0	0.0630	0.4855	0.1235

values

$$y_n = y(x_n) = \frac{1}{2} \log \left(\sum_m \left| \frac{d\mathrm{prob}_n}{dJ_{m,m+1}} \frac{1}{1 - \mathrm{prob}_n} \right|^2 \right),$$

where $J_{m,m+1}$ is the m-$(m+1)$ spin coupling strength and the sum is extended over all couplings. In our data base, N ranges from 114 up to 1998. The set of pairs is divided into I groups, $\{(X_i, Y_i)\}_{i=1}^{I}$, where we took $I = 3, 10, 100$.

For each data set $\{x_n, y_n\}_{n=1}^{N}$ corresponding to a certain number of spins and a certain $|\mathrm{IN}\rangle \to |\mathrm{OUT}\rangle$ transfer, the JT statistic Z and the p value were computed using the Matlab `JTtrend` function [7]. From the p value, a "reject/accept" decision on the Null Hypothesis H_0 of no trend was taken consistently with a significance level $\alpha = 0.05$. The average results over all case studies are shown in Table 1.

From Table 1 the following conclusions can already be drawn:

1. There is not much difference between the $I = 3$, 10 and 100 (number of bins) cases, except for the outlier $\min \mathrm{JT} = 0.364$, $I = 100$. The problem is that the data set contains controllers for a $(M, |\mathrm{OUT}\rangle)$ case-study and that this case-study has a sample set of only $N = 150$ controllers. Clearly, the arrangement of the $\{(x_n, y_n)\}_{n=1}^{150}$ data in "bins" of 100 defeats the purpose of robustification of the results by arguing on the medians of the bins. For this particular case, it turns out that the two medians do not conform to the rest of the results. Note that there is another $N = 114$ case-study, but for that one the 2 medians conform with the other results.

2. The mean p-value is borderline between "accept" H_0 (no disagreement with classical limitations) and "reject" H_0 (disagreement with classical limitations), with a slight tipping of the balance toward "reject." (Recall that $\alpha = 0.05$.)

3. $\min p = 0$ (up to 4 decimals) means that there are cases in strong disagreement with classical limitations—the log sensitivity increases with the error.

4. $\max p \approx 0.48 \gg 0.05$ means that there are cases where there is not enough evidence to disagree with the classical limitations—meaning that the log sensitivity does not have trend relative to an increase error.

5. Comparing Kendall τ with Jonckheere-Terpstra it is absolutely obvious that $\bar{p}_{\mathrm{Jonckheere-Terpstra}} \ll \bar{p}_{\mathrm{Kendall}\ \tau}$. Clearly the Jonckheere-Terpstra test implicitly filters the oscillatory logarithmic sensitivity data and renders a result with significantly higher confidence than the Kendall τ.

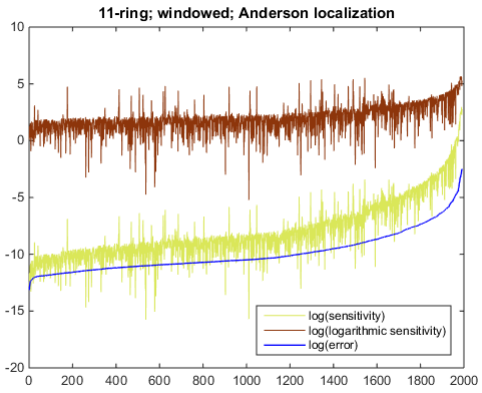

Figure 6: Sensitivity, logarithmic sensitivity, and error plotted on a logarithmic scale (for better comparison) versus index n of controller (2000 of them) for Anderson localization around spin 1 in an 11-ring. All 3 figures of merit are concordant, indicating that Anderson localization is anti-classical.

The upshot is that a simple relation like the classical $S + T = I$ cannot, in general, be expected in the quantum transport setup—except for the Anderson localization case, that is, holding a state of excitation at a single spin, or securing a successful "transfer" $|1\rangle \to |1\rangle$. In this case indeed p is consistently vanishing up to 4 decimals, rejecting the no trend hypothesis in the log sensitivity and pointing towards an increase of the log sensitivity with the error. This anti-classical behavior is not surprising, as the Anderson localization is probably the quantum transport case that most significantly departs from classical concepts.

6.3 Case studies

6.3.1 Case-study: Anderson localization: "reject" classical limitation

We consider the case of an 11-ring with the $|1\rangle \to |1\rangle$ "transfer." Fig. 6 shows that the various figures of merit are not conflicting—quite to the contrary, they are consistent. The detail of the experiment is shown in Table 2. Clearly, the "reject" decision is consistent with the visual appearance of the log sensitivity plot.

Table 2: Details of the 11-ring Anderson localization experiment on Jonckheere-Terpstra test of Null Hypothesis of no trend between error and logarithmic sensitivity

I	Kendall tau	$\lvert Z\rvert$	p	Null Hypothesis
3	0.4483	26.5509	0	"rejected"
10	0.4483	29.5768	0	"rejected"
100	0.4483	29.8896	0	"rejected"

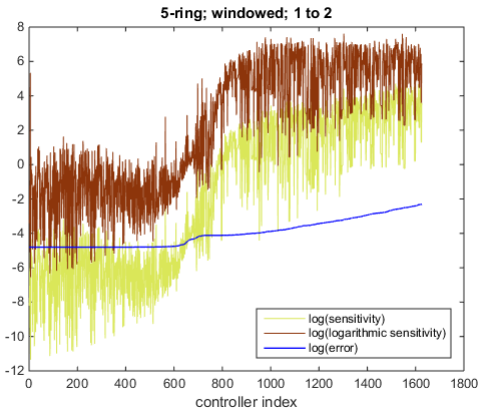

Figure 7: Sensitivity, log-sensitivity, and error plotted on a logarithmic scale versus index n of controller (1600 of them) for $|1\rangle \to |2\rangle$ transport in a 5-ring. Observe the strong concordance between the sensitivity and the log-sensitivity. Even though the concordance with the error is weaker, it still indicates anti-classical behavior.

Table 3: Details of the 5-ring under $|1\rangle \to |2\rangle$ transport experiment on Jonckheere-Terpstra test of Null Hypothesis of no trend between error and logarithmic sensitivity

I	Kendall tau	$\lvert Z\rvert$	p	Null Hypothesis
3	0.58	33.0028	0	"rejected"
10	0.58	34.7227	0	"rejected"
100	0.58	35.0389	0	"rejected"

6.3.2 Case study: "reject" classical limitation

Anderson localization is not the only case where an anti-classical behavior is observed, as shown by the strongly increasing trend of the log sensitivity in the case of a 5-ring under $|1\rangle \to |2\rangle$ transport shown in Figure 7. The details of the analysis is shown in Table 3.

6.3.3 Case-study: borderline "accept/reject" classical limitation

As "borderline" case, we choose a 14-ring with $|1\rangle \to |6\rangle$ transfer. The log sensitivity plot of Fig. 8 shows first an increasing trend and then a decreasing trend relative to the error, which explains the mixed "accept/reject" decision shown in Table 4.

6.3.4 Case study: "accept" classical limitation

Here we consider one of the best illustrative case of no increase of the log sensitivity. We consider the case of a 15-ring with the $|1\rangle \to |6\rangle$ transfer. Fig. 9 shows that the

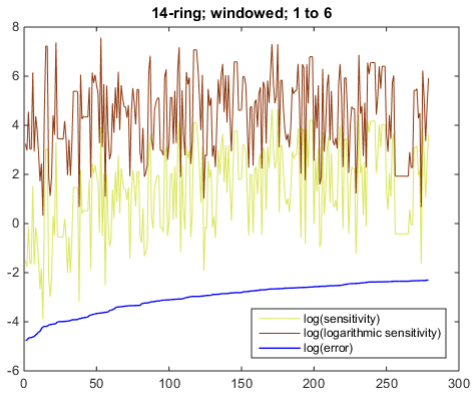

Figure 8: Sensitivity, log-sensitivity and error plotted on a logarithmic scale versus index n of controller (260 of them) for a 14-ring under $|1\rangle \to |6\rangle$ transport. While the error and sensitivity are concordant, the error and log-sensitivity are marginally concordant, because of the decreasing trend of the log-sensitivity as of controller 200.

Table 4: Details of the 14-ring $|1\rangle \to |6\rangle$ transport experiment on Jonckheere-Terpstra test of Null Hypothesis of no trend between error and logarithmic sensitivity (Recall that $\mathrm{JT}_{\alpha=0.05} \approx 1.6557$.)

I	Kendall tau	$\lvert Z\rvert$	p	Null Hypothesis
3	0.0575	1.4875	0.0684	"accept"
10	0.0575	1.5144	0.065	"accept"
100	0.0575	1.6696	0.0475	"reject"

logarithmic sensitivity has no trend compared with the error, as confirmed by the details of Table 2 and the "admit" the Null Hypothesis decision.

7 Results—Type II error and power of test

We compute the power of the Jonckheere-Terpstra test for α in a neighborhood of the 0.05 significance level decided upon in the previous sections, and in the generic experimental situation where $M = 1000$ and $I = 10$. We set α, compute the variance from (10), compute the critical $|Z|_\alpha$ by setting $p = \alpha$ in Eq. (11), and finally compute β_α from (12). The results are shown in Fig. 10. In order to acheive the "gold standard" of 80% power of the test, we need to have $\mu^A_{|Z|} \geq 2.5$, which is certainly achieved for the cases shown in Tables 2 and 3 where trends are detected.

We also considered the power of the Jonckheere-Terpstra test for various number M of spins, for various number I of "bins," to conclude that the power is not visibly affected by those quantities.

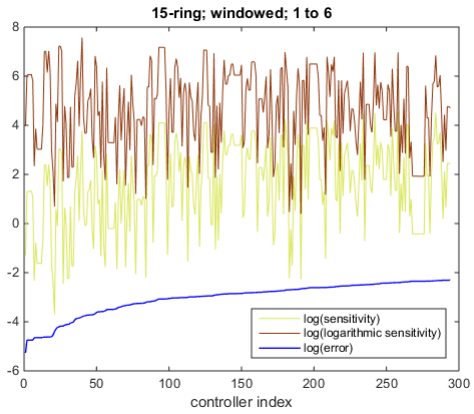

Figure 9: Sensitivity, log-sensitivity, and error plotted on a logarithmic scale versus index of controller (290 of them) in a 15-ring under $|1\rangle \to |6\rangle$ transport. While the sensitivity and the error are concordant, the log-sensitivity shows no trend—even possibly a slightly decreasing trend—versus n indicating rather classical behavior.

Table 5: Details of the 15-ring $|1\rangle \to |6\rangle$ transport experiment on Jonckheere-Terpstra test of Null Hypothesis of no trend between error and logarithmic sensitivity

I	Kendall tau	$\lvert Z\rvert$	p	Null Hypothesis
3	-0.0285	0.1789	0.4290	"accept"
10	-0.0285	0.7549	0.2252	"accept"
100	-0.0285	0.2052	0.4200	"accept"

8 Discussion: Dependency of error versus log-sensitivity relation on $(|\mathrm{IN}\rangle, |\mathrm{OUT}\rangle)$

In the previous study, the data incorporated *all* cases, up to symmetry, of $|\mathrm{IN}\rangle \to |\mathrm{OUT}\rangle$ transfers, for all M ranging from 3 to 20, with an overall positive concordant trend between error and log sensitivity. Here we examine how much the classical/anti-classical behavior depends on the relative position of the $|\mathrm{IN}\rangle$ and $|\mathrm{OUT}\rangle$ spins. The overall Jonckheere-Terpstra $|Z|$-data with $|\mathrm{IN}\rangle = |1\rangle$ of Section 6.2 is divided into three $|\mathrm{OUT}\rangle$-groups ($I = 3$) that roughly correspond to a decomposition of the right-half of the ring into 3 equally-sized sectors:

- Y_1: JT-data of $(120^\circ < \mathrm{angle}(|1\rangle, |\mathrm{OUT}\rangle) < 180^\circ + \epsilon)$,
- Y_2: JT-data of $(60^\circ < \mathrm{angle}(|1\rangle, |\mathrm{OUT}\rangle) < 120^\circ)$,
- Y_3: JT-data of $(0^\circ < \mathrm{angle}(|1\rangle, |\mathrm{OUT}\rangle) < 60^\circ)$,

as illustrated in Fig. 11. If M is not divisible by 3, we arrange the M-spin data such that $|Y_3| \geq |Y_2| \geq |Y_1|$ with at least a strict inequality. The more specific grouping of

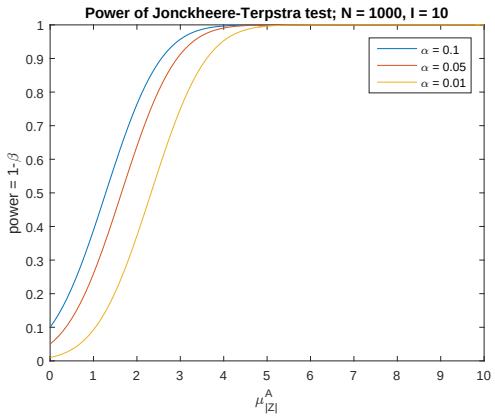

Figure 10: Power of Jonckheere-Terpstra test for various α's versus mean $\mu^A_{|Z|}$ under Alternative Hypothesis

Table 6: Contingency table of data: $[M : M'] - [|\text{OUT}\rangle : |\text{OUT}\rangle']$ denotes all Z-data, $I = 3$, pertaining to a number of spin between M and M' with initial spin state $|\text{IN}\rangle = |1\rangle$ and target spin state ranging from $|\text{OUT}\rangle$ to $|\text{OUT}\rangle'$.

Y_1	Y_2	Y_3
10-5	$[10 : 12] - [3 : 4]$	$[10 : 12] - [1 : 2]$
$[11 : 12] - [5 : 6]$	$[13 : 14] - [4 : 5]$	$[13 : 18] - [1 : 3]$
$[13 : 14] - [6 : 7]$	$[15 : 18] - [4 : 6]$	$[19 : 20] - [1 : 4]$
$[15 : 16] - [7 : 8]$	$[19 : 20] - [5 : 7]$	
$[17 : 18] - [7 : 9]$		
$[19 : 20] - [8 : 10]$		

the data is shown in the contingency Table 6.

With the JT-data arranged in the Y_1, Y_2, and Y_3 bins, we examine whether there is a trend in the JT data across the three bins. The Jonckheere-Terpstra test rejects the Null Hypothesis of no trend with $|Z| = 7.6283$ and $p = 0.0000$ (up to 4 decimals) for the Alternative Hypothesis of a trend $\tilde{Y}_1 \leq \tilde{Y}_2 \leq \tilde{Y}_3$, with at least one strict inequality. Therefore, when the spins of excitation transfer $|\text{IN}\rangle \to |\text{OUT}\rangle$ are not too far apart, the design behaves anti-classically (error and log sensitivity increase together). When they become nearly anti-podal, then the design behaves classically with the conflict between error and log sensitivity.

Note that this conclusion is supported *by the available dataset,* which contains only those controllers with a largest error of 0.1. This in particular means we have fewer controllers for the longer distance transitions on the ring, as it was considerably harder to find these. Possibly the conclusion could be invalidated by better optimizers able to find better controllers at long distance transport.

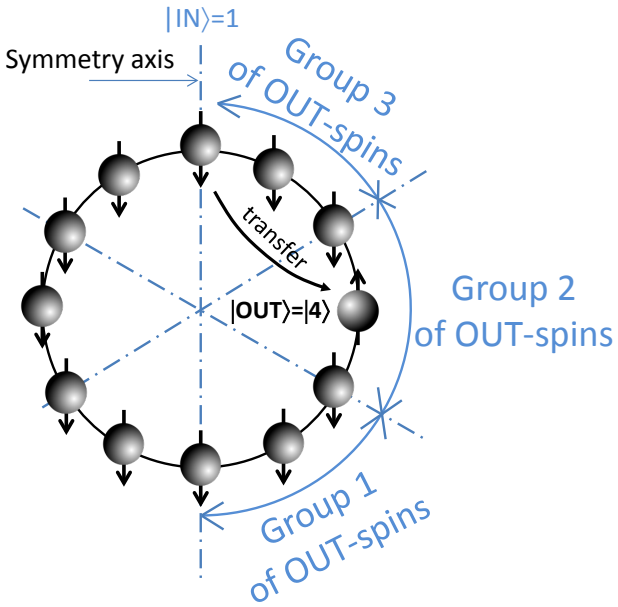

Figure 11: The 3 groups of |OUT⟩-data to assess dependency classical/anti-classical behavior on |OUT⟩-position around the ring

9 Conclusion & Future research directions

As already observed in [33], the quantum transport problem can be re-formulated in the classical control setup only at the expense of a complicated sensitivity matrix $\mathcal{S}(s)$ that embodies the projectivity of the quantum tracking error. Given the projective sensitivity matrix $\mathcal{S}(s)$, the fundamental limitations, if any, are not easy to come by. Here we have developed a statistical approach based on a sample set [25] of numerically optimized controllers. Precisely, for *every* ring from 3 to 20 spins and *every* transfer on such ring, a fairly large data set of locally optimal controllers, arranged by increasing order of their transfer errors, was constructed [24, 25]. With the controllers at hand, we investigated whether the logarithmic sensitivity anti-classically increases with the error using the Kendall tau and the Jonckheere-Terpstra tests, with a preference for the latter as it gives higher confidence. Out of all case-studies constructed from the whole dataset [25], it appears that there are cases that clearly show anti-classical behavior (H_0 rejected), while others show classical behavior (H_0 accepted). The former—rejection of no trend in favor of an increasing trend—is a challenge to the classical limitations that say that the error and the logarithmic sensitivity should be in conflict. By a further analysis, it was shown that for transfers between nearby spins, the classical limitation does not hold, while it tends to be recovered for transfers between distant spins.

The results derived here are based on a data set that retains, among other numerically optimized controllers, only those achieving a probability error no greater than 0.1.

The issue of large as opposed to differential parameter variations is addressed in [19,

31], where a structured singular value argument proves that challenge to the classical limitation remains in force. Note that [31] not only considers coupling errors but also field focusing errors and that the same μ-analysis argument [19, 31] is able to cope with initial state preparation errors. But a more challenging robustness problem consists in evaluating the classical limitation in the context of the gap between a model like (2) and some real-life quantum components, like some Copper compounds [29], which approach the Heisenberg model (2), but will never quite match the model. The same challenge applies to the DiVincenzo architecture [27] versus its models.

Finally, observe that all that precedes applies to coherent quantum dynamics. However, when the ring is subject to collective dephasing, the classical limitations tend to re-appear [34].

Acknowledgment

The authors wish to thank Professor Stanislav Minsker, Department of Mathematics, University of Southern California, for drawing our attention to the Type II error. Many thanks to Capt. Sean O'Neil, US Military Academy, for drawing our attention to the Stouffer test. Sophie Schirmer and Frank Langbein are supported by the Ser Cymru NRN AEM grant 82.

A Some related tests

There are many extensions/refinements of the Jonckheere-Terpstra test [35]. In case of small data sets, a modified version of (9) is proposed as

$$U_{ij} = (j-i)\sum_{k=1}^{N_i}\sum_{\ell=1}^{N_j}\Phi(Y_j(\ell) - Y_i(k)), \quad i<j.$$

Another recently proposed version [35] is

$$U_{ij} = (r_{j\ell} - r_{ik})\sum_{k=1}^{N_i}\sum_{\ell=1}^{N_j}\Phi(Y_j(\ell) - Y_i(k)), \quad i<j,$$

where $r_{j\ell}, r_{ik}$ denote the position (rank) of $Y_j(\ell), Y_i(k)$ in the combined data. Finally, yet another extension proposes a confidence interval [30].

It was observed that the first refinement of the Mann-Whitney U-statistic does not change the overall results and conclusion.

B Left-tailed Jonckheere-Terpstra test

In case the classical limitations are likely to hold, the Jonckheere-Terpstra test should be organized around the Alternative Hypothesis

$$\widetilde{Y}_1 \geq \widetilde{Y}_2 \geq ... \geq \widetilde{Y}_I,$$

that is, the log sensitivity is decreasing with increasing error. The test is analogous to the classical one, but in the opposite tail. Rejection of the Null Hypothesis in favor of the above Alternative Hypothesis is more likely to happen with the instantaneous performance optimizing controllers. This is left to a further paper.

C (Rank) von Neumann test

A qualitative argument in favor of the randomness of the results of the search algorithm was presented in Sec. 6.1.1, but a quantitative analysis stills needs to be set up.

C.1 von Neumann ratio test

The genesis of the von Neumann test [42, 43] is to decide whether a trend exists in a series of observation $\{y_n\}_{n=1}^N$ *totally* ordered by the variable n, usually thought to be the time. The von Neumann test of independence relies on the paradigm that a trend compromises the randomness of a time-series. To quantify this observation, define the mean square successive difference

$$\delta^2 = \frac{1}{N-1}\sum_{n=1}^{N-1}(y_{n+1}-y_n)^2$$

and the (slightly biased) variance estimate

$$s^2 = \frac{1}{N}\sum_{n=1}^{N}(y_n-\bar{y})^2, \quad \left(\bar{y} = \frac{1}{N}\sum_{n=1}^{N} y_n\right).$$

The von Neumann ratio is defined as

$$\mathrm{VN} = \frac{\delta^2}{s^2}.$$

Taking y_n linear in n, hence giving y_n a trend, it is easy to see that $\lim_{N\to\infty}\delta^2/s^2 \to 0$. Intuitively, small VN means trend and large VN means independence. Precisely, von Neumann [42, 43] demonstrated that under the assumption of normality and independence, $E(\mathrm{VN}) = 2N/(N-1)$, so that 2 can be taken as threshold value for large sample size. In [38], an empirical distribution for VN was derived, appearing normal with mean 2 for large N. Critical values of the left-tailed test of the Null Hypothesis of independence are derived in [38, Table 1].

The problem is that, as observed in [4], this test is not robust against deviation from normality in the data. We therefore have to resort to a nonparametric test.

C.2 Rank von Neumann ratio test

The nonparametric von Neumann test does not rely on numerical values of the observations, but on their ranking. The log sensitivity observations are ranked consistently with increasing error. To be specific, let x_n be the error and y_n the log-sensitivity with

"time-stamp" n in bin i. Let $\pi_i : \{1, ..., N_i\} \to \{1, ..., N_i\}$ be the permutation of the set of N_i labels such that $x_{\pi_i(n)}$ is nondecreasing. The $y_{\pi_i(n)}$ sequence may have an overall nondecreasing trend in case the classical limitation is violated, but it is not uniformly nondecreasing. We show randomness in the latter sequence. We define r_n to be the rank of the observation $y_{\pi_i(n)}$ in a nondecreasing reordering of the data $\{y_n\}$. Inside the bin $i \in I$, the *rank* von Neumann ratio is

$$\mathrm{RVN}_i = \frac{\sum_{n=1}^{N_i-1}(r_n - r_{n+1})^2}{\sum_{n=1}^{N_i}(r_n - \bar{r}_i)^2}, \quad \left(\bar{r}_i = \frac{1}{N_i}\sum_{n=1}^{N_i} r_n\right).$$

The statistic of the RVN is approximately β-distributed, from which the left-tailed critical values of RVN_α are cataloged in [4, Table 2]. Naturally, in case the classical limitation is challenged, some correlation should be expected as the data $\{y_n\}$ is on the average increasing. For this reason, before running the von Neumann test, the "trend" should be removed.

For example, consider a 7-ring with target spin 3, and 15 groups for a total of 1515 observations. From [4, Table 2] of the thresholds of the β-function statistic, and observing that each group contains about 100 observations, any value ≥ 1.67 would indicate randomness with 95% confidence. The data $\{y_n\}_{n=1}^{N_i}$ is detrended with the `detrend` function of Matlab, which removes the best overall linear fit of the trend from the data in bin i. Repeating this for all bins, the rank von Neumann ratio test for all 15 bins yields

RVN =

2.1908 1.8130 2.1426 1.7964 1.7150 2.0761 1.3343 1.9043 1.7925 1.2026

1.8994 2.0175 1.9932 1.8010 1.8657

Observe that 13 out of 15 bins are beyond the threshold of 1.67, reinforcing our claim of randomness in the data.

References

[1] H. Abdi. The Kendall rank correlation coefficient. In N. Salkind, editor, *Encyclopedia of measurements and Statistics*. Sage, Thousand Oaks, CA, 2007.

[2] P. W. Anderson. Absence of diffusion in certain random lattices. *Physical Review*, 109(5):1492–1505, March 1958.

[3] M. Araki and H. Taguchi. Two-degree-of-freedom PID controllers. *International Journal of Control, Automation, and Systems*, 1(4), December 2003.

[4] R. Bartels. The rank version of von Neumann's ratio test for randomness. *Journal of the American Statistical Association*, 77(377):40–46, March 1982.

[5] P. Bogdan, E. Jonckheere, and S. Schirmer. Multi-fractal geometry of finite networks of spins: Nonequilibrium dynamics beyond thermalization and many-body-localization. *Chaos, Solitons & Fractals*, 103:622–631, October 2017. available at arXiv:1608.08192 [quant-ph].

[6] Amy Buros, Jack D. Tubbs, and Johanna S. Van Zyl. Application of AUC regression for the Jonckheere trend test. *Statistics in Biopharmaceutical Research*, 9(2):147–152, 217. Available at http://dx.doi.org/10.1080/19466315.2016.1265581.

[7] G. Cardillo. Jonckheere-Terpstra test: A nonparametric test for trend. Available at http://www.mathworks.com/matlabcentral/fileexchange/22159, 2008.

[8] W. B. Dong, R.-B.Wu, W. Zhang, C. W. Li, and T. J. Tarn. Spatial control model and analysis of quantum fields in one-dimensional waveguides. *SIAM Journal on Control and Optimization*, 54(3):1352–1377, 2016.

[9] David L. Elliott. *Bilinear Control Systems—Matrices in Action*, volume 169 of *Applied Mathematical Series*. Springer, Dordrecht, Heidelberg, London, New York, 2009.

[10] P. Griffiths and J. Harris. *Principles of Algebraic Geometry*. Wiley Classic Library. Wiley, New York, 1994.

[11] K. H. Hamed. The distribution of Kendall's tau for testing the significance of cross-correlation in persistent data. *Hydrological Sciences Journal*, 56(5):841–853, 2011. doi: 10.1080/02626667.2011.586948.

[12] I. M. Horowitz. *Synthesis of Feedback Systems*. Academic Press, New York, London, 1963.

[13] Dirk Hundertmark. A short introduction to Anderson localization. In *Proceedings of the LMS Meeting on Analysis and Stochastics of Growth Processes and Interface Models*, pages 194–218. Oxford University Press, Oxford, United Kingdom, 2008.

[14] A. Jonckheere. A distribution-free k-sample test against ordered alternatives. *Biometrika*, 41:133145, 1954. doi:10.2307/233301.

[15] E. Jonckheere, F. C. Langbein, and S. G. Schirmer. Curvature of quantum rings. In *Proceedings of the 5th International Symposium on Communications, Control and Signal Processing (ISCCSP 2012)*, Rome, Italy, May 2-4 2012. DOI: 10.1109/ISCCSP.2012.6217863.

[16] E. Jonckheere, S. Schirmer, and F. Langbein. Geometry and curvature of spin network. In *2011 IEEE Multi-Conference on Systems and Control*, pages 786–791, Denver, CO, September 2011. DOI: 10.1109/CCA.2011.6044395. Available at arXiv:1102.3208v1 [quant-ph].

[17] E. Jonckheere, S. Schirmer, and F. Langbein. Quantum networks: The anticore of spin chains. *Quantum Information Processing*, 13:1607–1637, 2014. Published on line May 24, 2014. (DOI: 10.1007/s11128-014-0755-5). Available at `http://eudoxus2.usc.edu`.

[18] E. Jonckheere, S. Schirmer, and F. Langbein. Information transfer fidelity in spin networks and ring-based quantum routers. *Quantum Information Processing (QINP)*, 14(10), 2015. DOI: 10.1007/s11128-015-1136-4; available at `http://eudoxus2.usc.edu` and arXiv:submit/1359959 [quant-ph] 24 Sep 2015.

[19] E. Jonckheere, S. Schirmer, and F. Langbein. Structured singular value analysis for spintronics network information transfer control. *IEEE Trans-*

actions on Automatic Control, December 2017. To appear, available at `http://eudoxus2.usc.edu` and arXiv:1706.03247v1 [quant-ph] 10 Jun 2017.

[20] M. G. Kendall. A new measure of rank correlation. *Biometrika*, 30(1-2):81–93, 1938.

[21] S. C. Kim, S. J. Lee, W. J. Lee, Y. N. Yum, J. H. Kim, S. Sohn, J. H. Park, J. Lee, J. Lim, and S. W. Kwon. Stouffer's test in a large scale simultaneous hypothesis testing. *PLoS ONE*, 8(5):e63290, May 2013.

[22] R. L. Kosut, M. D. Grace, and C. Brif. Robust control of quantum gates via sequential convex programming. *Phy. Rev. A*, 88:052326, 2013.

[23] A. Lagendijk, B. van Tiggelen, and D. Wiersma. Fifty years of Anderson localization. *Physics Today*, 62:24–28, August 2009.

[24] F. Langbein, S. Schirmer, and E. Jonckheere. Time optimal information transfer in spintronics networks. In *IEEE Conference on Decision and Control*, pages 6454–6459, Osaka, Japan, December 2015.

[25] Frank C. Langbein, Sophie G. Schirmer, and Edmond Jonckheere. Static bias controllers for XX spin-1/2 rings. Data set, `figshare`, DOI:10.6084/m9.figshare.3485240.v1, July 3 2016.

[26] E. Letn and P. Zuluaga. A note on the variances of the tests of Kendall, Jonckheere, and Terpstra. *Communications in Statistics - Theory and Methods*, 36(5):927–937, 2007.

[27] D. Loss and D. DiVincenzo. Quantum computing with quantum dots. *Physical Review Letters*, A 57(1):120–126, January 1998.

[28] R. Luesink and H. Nijmeijer. On the stabilization of bilinear systems via constant feedback. *Linear Algebra and Its Applications*, 122/123/124:457–474, 1989.

[29] J. M. Maillet. Heisenberg spin chains: from quantum groups to neutron scattering experiments. *Séminaire Poincaré*, X:129–177, 2007.

[30] J. W. McKean and J. Naranjo. A robust method for the analysis of experiments with ordered tratment levels. *Psychological Reports*, 89:267–273, 2001.

[31] S. O'Neil, E. Jonckheere, S. Schirmer, and F. Langbein. Sensitivity and robustness of quantum rings to parameter uncertainty. In *IEEE CDC*, Melbourne, Australia, December 2017. To appear, available at arXiv:1708.09649v1.

[32] M. G. Safonov, A. J. Laub, and G. L. Hartmann. Feedback properties of multivariable systems: The role and use of the return difference matrix. *IEEE Transactions on Automatic Control*, AC-26(1):47–65, February 1981.

[33] S. Schirmer, E. Jonckheere, and F. Langbein. Design of feedback control laws for spintronics networks. *IEEE Transactions on Automatic Control*, 2017. To appear; available at arXiv:1607.05294.

[34] S. Schirmer, E. Jonckheere, S. O'Neil, and F. Langbein. Emergence of classicality under decoherence in robust quantum control. Available at http://eudoxus2.usc.edu, 2017.

[35] Guogen Shan, Daniel Young, and Le Kang. A new powerful nonparametric rank test for ordered alternative problem. *Plos One*, 9:1–10, November 2014. e112924.

[36] G. P. Sillito. The distribution of Kendall's τ coefficient of rank correlation in rankings containing tie. *Biometrika*, 34(1/2):36–40, January 1947.

[37] S. A. Stouffer, E. A. Suchman, L. C. DeVinney, S. A. Star, and R. M. Williams. *The American Soldier, Vol 1: Adjustment during Army Life*. Princeton University Press, Princeton, 1949.

[38] R. K. Swihart and N A. Slade. Testing for independence of observations in animal movements. *Ecology*, 66(4):1176–1184, 1985.

[39] T. J. Terpstra. The asymptotic normality and consistency of Kendall's test against trend, when ties are present in one ranking. *Indagationes Mathematicae*, 14:327333, 1952.

[40] K. Tsuyuzaki. Stouffer.test: Stouffer weighted Z-score (inverse normal method). Available at: https://www.rdocumentation.org/packages/metaSeq/versions/1.12.0/topics/Stouffer.test.

[41] P. D. Valz and A. I. McLeod. A tremendously simplified derivation of the variance of Kendall's τ. Available at `http://www.stats.uwo.ca/faculty/aim/vita/ps/kendall.pdf`.

[42] J. von Neumann. Distribution of the ratio of the mean square successive difference to the variance. *Ann. Math. Statist.*, 12(4):367–395, 1941.

[43] J. von Neumann, R. H. Kent, H. R. Bellinson, and B. I. Hart. The mean square successive difference. *The Annals of Mathematical Statistics*, 12:153–162, 1941.

[44] M. C. Whitlock. Combining probability from independent tests: the weighted z-methods is superior to Fisher's approach. *J. Evol. Biol.*, 18:1368–1373, 2005.

[45] Yangmin Xie and Andrew Alleyne. Robust two degree-of-freedom control of MIMO system with both model and signal uncertainties. In *19th World Congress*, pages 9313–9320, Cape Town, South Africa, August 24-29 2014. The International Federation of Automatic Control (IFAC).